Spherical Shock Waves of Variable Energy in A Radiating Atmosphere

[1]R K Anand, [2]H C Yadav

[1]Department of Physics, UGC Centre of Advanced Studies, University of Allahabad, Allahabad 211002, India

[2]Department of Physics, CMP College, Allahabad 211002, India

anand.rajkumar@rediffmail.com, harish0chandra@gmail.com

Abstract

This paper presents power series similarity solutions for spherical shock waves of variable energy propagating in a radiating gas, taking into consideration the Rosseland's radiative diffusion model. These similarity solutions are obtained for an energy input $E = E_o\, t^{4/3}$, where E is the energy released up to time *t* and E_o is a functional constant. The effects of radiation-parameter are explored on the pressure, the density, the particle velocity and the heat flux of radiation just behind the spherical shock front. The results provided a clear picture of whether and how the radiation flux affects the distribution of the flow variables in the region behind the spherical shock waves.

Keywords: Shock Waves, Variable Energy, Radiation Heat Flux, Power Series Similarity Solutions

PACS Numbers: 47.40−X, 52.35.Tc, 47.40. Nm

1. Introduction

At very high temperatures radiation phenomena can significantly modify the flow field behind the shock waves due to the interaction of radiation with matter. The effects of radiation on shock dynamics are of interest to many areas of space research, nuclear and high energy density physics and are of particular importance for the understanding of astrophysical shocks. The shock waves play an important role in the evolution of interstellar medium providing a source of energy and triggering various phenomena including star formation. Supernovae are a common source of such strong shock waves, which expand into the surrounding of the interstellar medium gathering up the material into a thin, dense shell. If the circumstellar medium is dense enough, transfer of radiation can play a significant role in the development of supernova remnant blast waves. Theoretical investigations confirm that strongly radiative situations lead to numerous consequences; these include the production of an ultraviolet driven ionization front ahead of the blast wave [1] and a blast wave front deceleration greater than a simple adiabatic blast wave due to energy depletion by radiative cooling [2]. These effects are believed to have important consequences on the development of supernova remnants.

It was Stokes [3] who first studied the effects of radiation on the sound waves. The effects of radiation on the shock waves were discussed briefly by Sachs [4], Guess and Sen [5] and Sen and Guess [6]. It is important to mention that the propagation of strong shock waves into a cold gas was investigated by Sachs [4] assuming the negligible effects due to radiation pressure and radiation energy ahead of the shock front. Guess and Sen [5] studied the shock waves in non-equilibrium radiative medium and examined the broadening of shock wave thickness by the radiation flux. The classic discussion of radiating shock waves was given by Zel'dovich and Raizer [7] and this discussion was repeated and extended very clearly by Mihalas and Mihalas [8]. Marshak [9] studied the effects of radiation on the shock wave propagation using the radiation diffusion model. Using the same model of radiation, Elliott [10] obtained a similarity solution for the shock waves initiated by a sudden release of energy due to high temperature attained at the center for an optically thick gas and opaque shock front. Considering the effects of thermal radiation in the case of general opacity (optically thick) and in the transparent (optically thin) limit, similarity solution for planar shock wave generated by a piston in a perfect gas was first obtained by Wang [11] and for cylindrical or spherical shock waves by Helliwill [12]. Similarity or non-similarity solution for the radiating shock waves in an exponential medium was also obtained by

Laumback and Probstein [13, 14], Bhowmick [15] and Singh and Srivastava [16]. Taking into consideration the effects due to conduction and radiation in the two limits of Rosseland radiation diffusion and Plank radiative emission, Ghoniem et al [17] obtained a self-similar solution for a spherical shock wave in an optically thick and thin gas. In view of the internal heat conduction and thermal radiation in a detonating medium, Gretler and Wehle [18] studied the propagation of blast waves with exponential heat release. Recently Anand [19] presented the similarity solutions in the form of power series for spherical shock waves with time dependent variable energy propagating in two-phase gas–particle medium.

Although the similarity solutions of shock waves in an ideal gas has been discussed very extensively in the literature, but the similarity solutions taking radiation into account have hardly been investigated. In astrophysical flows, radiation often contains a large fraction of the energy density, momentum density, and stress i.e., pressure in the radiating fluids. Moreover, radiative transfer is usually the most effective energy-exchange mechanism within the radiating fluids. However, theoretical study of such problems becomes very complex when the similarity models for blast waves take radiation effects into account. In treating radiative effects attention has been focused exclusively on radiative energy exchange, and both the effects of radiative forces and the dynamics of the radiation field itself have been ignored. A radiation driven explosion is produced when large amount of radiant energy is released nearly instantaneously from the point source in a cold gas. The radiation path ionizes and strongly heats the gas and can thus drive violent hydrodynamic phenomena. When a shock wave is propagated through a gas occupying a large volume, and the dimensions of the heated region are very large in comparison with the mean free path of a photon so that the gas temperature changes very little over a distance of the order of mean free path, the thermal equilibrium in a wave is brought into local thermodynamic equilibrium with the fluid. The radiative equilibrium also exists immediately behind the shock front.

To our best knowledge, so far there is no paper reporting the power series similarity solutions for radiating shock waves taking into consideration the Rosseland's radiative diffusion model [20]. Energy loss via radiation also affects the density behind the shock front, and can lead to compression ratios far greater than the maximum compression ratio possible at the shock front itself. In the present research paper, the power series similarity solutions are obtained up to third approximation for spherical shock wave of variable energy propagating in a radiating gas, taking into consideration the Rosseland's radiative diffusion model. The total energy input is assumed to vary with time according to $E = E_0 t^k$ where E_0 and k are constants [21]. It is further assumed that the released energy is totally absorbed immediately behind the shock front where the density is relatively high. For the energy input parameter $k = 0$, the case of classical point explosion is found as a limiting case which is initiated by a sudden release of a constant amount of energy $E = E_0$ at time $t = t_0$. For $k = 1$, incident laser radiation is absorbed at constant rate E_0. It is notable that the radiation pressure and radiation energy are considered to be very small in comparison to material pressure and energy respectively, and therefore, in the present investigation only the radiation flux is taken into consideration. For this purpose, a model is developed to provide a simplified and complete treatment of the propagation of variable energy spherical shock waves in a radiating fluid. It is worth mentioning that the effects due to the radiation enter through the radiation-parameter. The numerical estimations of the flow quantities behind the spherical shock front are carried out using the MATHEMATICA and MATLAB codes. The present model appropriately makes obvious the effects due to an increase in (i) the propagation distance from the shock front, (ii) the radiation parameter and (iii) the inverse of square of Mach number, on the pressure, the density, the particle velocity and the radiation heat flux just behind the spherical shock front. The results provided a clear picture of whether and how the radiation-parameter and the inverse of square of Mach number affect the flow field just behind the radiating shock front. The paper is structured as follows. The background information is provided in Section 1 as an introduction. Section 2 contains the general assumptions and notations. The similarity transformation and energy integral equation are discussed in Section 3. In Section 4 power series similarity solutions are presented. Section 5 mainly describes numerical results with discussion on the important components of the present model. Finally, the conclusions are drawn in Section 6.

2. Basic Equations and Boundary Conditions

The non-steady, one dimensional flow field in a radiating gas is a function of two independent variables; the time *t* and the space coordinate *r*. In order to get some essential features of radiating shock wave propagation, it is assumed that the equilibrium flow condition is maintained in the flow field. The conservation equations governing the flow of a one-dimensional, inviscid, ideal gas with radiation heat flux under an equilibrium condition can be expressed conveniently in Eulerian coordinates as follows:

$$\frac{\partial u}{\partial t} + u\frac{\partial u}{\partial r} + \frac{1}{\rho}\frac{\partial p}{\partial r} = 0 \qquad (1)$$

$$\frac{\partial \rho}{\partial t} + u\frac{\partial \rho}{\partial r} + \rho\,(\frac{\partial u}{\partial r} + j\frac{u}{r}) = 0 \qquad (2)$$

$$\frac{\partial p}{\partial t} + u\frac{\partial p}{\partial r} + \gamma\, p\,(\frac{\partial u}{\partial r} + j\frac{u}{r}) + (\gamma-1)\frac{\partial q}{\partial r} + jq\frac{(\gamma-1)}{r} = 0 \qquad (3)$$

where $\rho(r,t)$ is the density, $p(r,t)$ is the pressure, $u(r,t)$ is the velocity at a distance *r* from the origin O, at time *t* and γ is the adiabatic index. The geometrical factor j is defined by $j = d\ln A/d\ln r$, where *A* is the flow cross-section area. Then the one-dimensional flow in plane, cylindrical and spherical symmetry is characterized by j = 0, 1, and 2, respectively. The equation of state for an ideal gas is $p = \Gamma\,\rho\,T$, where, Γ is a gas constant. Assuming local thermodynamic equilibrium and taking the Rosseland's radiative diffusion model [20], we can write

$$q = -(1/3)\, c\mu\, \partial(\sigma T^4)/\partial\, r \qquad (4)$$

where $\sigma\, c/4$ is the Stefan-Boltzmann constant; *c*, is the velocity of light and μ, is the mean-free path of radiation. Following Wang [21], the mean free path is given as: $\mu = \mu_o \rho^{\alpha'} T^{\beta'}$; where, μ_o, α', and β' are constants. The speed of sound *a*, in unperturbed state is given as: $a_o^2 = p_o/\rho_o$, where p_o and ρ_o are pressure and density in unperturbed state, respectively. The flow field is bounded by two boundaries: viz., the shock front and inner expanding surface (piston). The downstream Mach number *M* is defined by $M = U/a_o$, where *U*, is the velocity of shock. The boundary conditions in terms of *M* are written as:

$$u = \left[1 - \frac{1}{\gamma M^2}\right] U$$

$$p = p_o M^2 \qquad (5)$$

$$\rho = \gamma\, \rho_o M^2$$

$$q = \frac{1}{2}\left[\frac{1}{\gamma^2 M^4} - 1\right]\rho_o U^3$$

The energy carried by the blast wave is equal to the energy supplied by the explosive and thus remains constant. Therefore, the principle of global energy can be expressed in terms of the following integral relation

$$E = n\int_{R_p}^{R}\left\{(u^2/2) + p/\rho(\gamma-1)\right\}\rho\, r^j dr - n\int_{o}^{R}(p_o/(\gamma-1))R^j dr \qquad (6)$$

where $n = 2j\pi + (j-1)(j-2)/2$, *R* is the shock radius and R_p is the position of piston. Basically, the Freeman's model [21] is independent of the condition whether the energy is absorbed at the shock front (laser radiation) or within the flow field where the energy is supplied by a driving piston as in the present problem. At the inner expanding surface, the kinematics condition is satisfied, requiring that $\left(dR_p/dt = u\right)_{r=R_p}$. In the present paper, the total energy of the flow-field behind the shock is not constant, but assumed to be time dependent and varying as:

$$E = E_o t^k \;,\; k \geq 0 \qquad (7)$$

where E_o is a functional constant and k is known as energy-input parameter.

3. Similarity Transformation and Energy Integral Equation

The basic equations can be made dimensionless by transforming the independent variables for space coordinate *r* and time coordinate *t* into new independent variables [19, 21, 23]

$$x = r/R,\; y = (a_o/U)^2 \qquad (8)$$

Here x and y are the so-called field co-ordinate and front co-ordinate, respectively. Now the other flow variables are non-dimensionalised by the following substitutions

$$\begin{aligned} &u = U\, f(x,y), \quad p = p_o\,(U/a_o)^2 g(x,y), \quad \rho = \rho_o\, h(x,y), \quad q = p_o a_o (U/a_o)^3 Q(x,y), \\ &t = t_o\, \omega, \quad R = R_o \xi \quad \text{and} \quad R_o = a_o\, t_o \end{aligned} \qquad (9)$$

where *f, g, h, Q,* ω and ξ are new non-dimensional variables. R_o and t_o are the characteristic length and time-related to the energy input by,

$$R_o = (E_o t_o^k / n\, p_o)^{1/(j+1)} \qquad (10)$$

With the aid of equations (7), (8) and (9), the flow equations (1-4); the boundary conditions (5) and the energy balance equation (6) can be written in non-dimensional form as:

Flow equations

$$(f-x)\,\partial f/\partial x + \xi\,\partial f/\partial\xi + (\xi\, f/U)\,\partial U/\partial\xi + 1/\gamma\, h = 0$$

$$(f-x)\,\partial h/\partial x + \xi\,\partial h/\partial\xi + h\,(\partial f/\partial x + j\, f/x) = 0 \qquad (11)$$

$$\begin{aligned}&(f-x)\,\partial g/\partial x + \xi\,\partial g/\partial\xi + (2\,\xi\, g/U)\,\partial U/\partial\xi + \gamma\, g\,(\partial f/\partial x + jf/x) + \\ &(\gamma-1)\,\partial Q/\partial x + j\,(\gamma-1)Q/x = 0\end{aligned}$$

$$\partial Q/\partial x + N\, y\,(h\,\partial g/\partial x - g\,\partial h/\partial x) = 0$$

where $N = -(4c\sigma\,\mu_o\rho_o^{3/2})/(3p_o\Gamma^{1/2})$ and is called a radiation-parameter.

Boundary conditions

$$f(1,y) = 1 - \frac{1}{\gamma M^2}$$

$$g(1,y) = 1 \tag{12}$$

$$h(1,y) = \gamma M^2$$

$$Q(1,y) = \frac{1}{2}\left[\frac{1}{\gamma^2 M^4} - 1\right]$$

Energy balance equation

$$\omega^k = \xi^{j+1}[J\ y^{-1} - 1/(j+1)(\gamma-1)]$$

$$\text{or } J\,\xi^{j+1} = y\,\omega^k + y\,\xi^{j+1}/(j+1)(\gamma-1) \tag{13}$$

where $J = \int_{x_p}^{1} (h\ f^2/2 + g/(\gamma-1))\ x^j dx$ and x_p being the piston position.

It is assumed that the functions f, g, h and Q can be expressed in the power series of y as:

$$f(x,y) = f_o(x) + y\ f_1(x) + y^2 f_2(x) + \ldots\ldots\ldots\ldots\ldots\ldots$$

$$g(x,y) = g_o(x) + y\ g_1(x) + y^2 g_2(x) + \ldots\ldots\ldots\ldots\ldots\ldots$$

$$h(x,y) = h_o(x) + y\ h_1(x) + y^2 h_2(x) + \ldots\ldots\ldots\ldots\ldots\ldots \tag{14}$$

$$Q(x,y) = Q_o(x) + y\ Q_1(x) + y^2 Q_2(x) + \ldots\ldots\ldots\ldots\ldots\ldots$$

Following the Freeman's model [21], we can write,

$$\xi = \xi_o\ y^{1/\lambda_o}(1 + \xi_1 y + \xi_2 y^2 + \ldots\ldots\ldots\ldots\ldots\ldots\ldots) \tag{15}$$

$$\omega = \{2\,\xi_o/(\lambda_o+2)\}y^{(\lambda_o+2)/2\lambda_o}(1 + \omega_1\xi_1 y + \omega_2\xi_2 y^2 + \ldots\ldots.) \tag{16}$$

$$J = J_o(1 + \sigma_1 y + \sigma_2 y^2 + \ldots\ldots\ldots\ldots\ldots) \tag{17}$$

where $\lambda_o = 2(j-k+1)/(2+k)$, $\omega_1 = (\lambda_o+1)(\lambda_o+2)/(3\lambda_o+2)$,

$\omega_2 = (\lambda_o+2)(2\lambda_o+1)/(5\lambda_o+2)$, $\omega_3 = (\lambda_o+2)(3\lambda_o+1)/(7\lambda_o+2)$.

Substituting (14-17) into energy equation (13) ensures its power series form provided $1/\lambda_o$ and $(\lambda_o+2)/2\lambda_o$ are positive integer, i.e., $1/\lambda_o = I$ (where, I is a positive integer). Which is equivalent to

$$k = 2\{I(j+1)-1\}/(2I+1). \tag{18}$$

It can be seen that for these values of k, the term $k(\lambda_o + 2)/2\,\lambda_o$ automatically becomes a positive integer. In this paper the first permissible value of k which is equal to 4/3, is used for computational work.

4. Power Series Similarity Solutions for Perturbed Flow

Now substituting equations (14) and (15) into the system of equations (11) and (12), and equating the coefficients of different power of y, we get for the zeroth power of y

$$\begin{gathered}
(f_o - x)\,h_o f_o' - 0.5 f_o h_o + g_o'/\gamma = 0 \\
2 f_o h_o/x + h_o f_o' - x\,h_o' + f_o h_o' = 0 \\
2\gamma\, f_o g_o/x - g_o - 2\,Q_o/x + 2\gamma\,Q_o/x + \gamma\,g_o f_o' - x\,g_o' + f_o g_o' - Q_o' + \gamma\,Q_o' = 0 \\
Q_o' = 0
\end{gathered} \tag{19}$$

$$f_o(1) = 1,\ g_o(1) = 1,\ h_o(1) = 0,\ Q_o(1) = -0.5 \tag{20}$$

For the first power of y, we find that

$$\begin{gathered}
0.5\xi_1 f_o h_o + f_1 h_o - 0.5(f_1 h_o + f_o h_1) + f_1 h_o f_o' + (f_o - x)\,(h_1 f_o' + h_o f_1') + g_1'/\gamma = 0 \\
2 f_1 h_o/x + h_1 + 2 f_o h_1/x + h_1 f_o' + h_o f_1' + f_1 h_o' - x h_1' + f_o h_1' = 0 \\
\xi_1 g_o + 2\gamma\, f_1 g_o/x + 2\gamma\, f_o g_1/x - 2Q_1/x + 2\gamma\,Q_1/x + \gamma\,g_1 f_o' + \\
\gamma\,g_o f_1' + f_1 g_o' - x\,g_1' + f_o g_1' - Q_1' + \gamma\,Q_1' = 0 \\
N\,h_o g_o' - N\,g_o h_o' + Q_1' = 0
\end{gathered} \tag{21}$$

$$f_1(1) = -1/\gamma,\ g_1(1) = 0,\ h_1(1) = 0,\ Q_1(1) = 0 \tag{22}$$

For the second power of y, we find that

$$\begin{gathered}
0.5(-2\xi_1^2 + 2\xi_2) f_o h_o - \xi_1 f_1 h_o + 2 f_2 h_o + f_1 h_1 + 0.5\xi_1(f_1 h_o + f_o h_1) - 0.5(f_2 h_o + \\
f_1 h_1 + f_o h_2) + f_2 h_o f_o' + f_1(h_1 f_o' + h_o f_1') + (f_o - x)(h_2\,f_o' + h_1 f_1' + h_o f_2') + g_2'/\gamma = 0 \\
2 f_2 h_o/x - \xi_1 h_1 + 2 f_1 h_1/x + 2h_2 + 2 f_o h_2/x + h_2 f_o' + h_1 f_1' + \\
h_o f_2' + f_2 h_o' + f_1 h_1' - x\,h_2' + f_o h_2' = 0 \\
-2\xi_1^2 g_o + 2\xi_2 g_o + 2\gamma\, f_2 g_o/x + 2\gamma\, f_1 g_1/x + g_2 + 2\gamma\, f_o g_2/x - \\
2Q_2/x + 2\gamma\,Q_2/x + \gamma\,g_2 f_o' + \\
\gamma\,g_1 f_1' + \gamma\,g_o f_2' + f_2 g_o' + f_1 g_1' - x\,g_2' + f_o g_2' - Q_2' + \gamma\,Q_2' = 0
\end{gathered} \tag{23}$$

$$N\, h_1 g_o^{'} + N\, h_o g_1^{'} - N\, g_1 h_o^{'} - N\, g_o h_1^{'} + Q_2^{'} = 0$$

$$f_2(1) = 0,\ g_2(1) = 0,\ h_2(1) = 0,\ Q_2(1) = 0.5/\gamma^2 \qquad (24)$$

4.1. First approximation solution

The system of equations (19) with boundary conditions (20) is now numerically integrated by Runge-Kutta-Method. The integration is started at the shock front and continued until a value x_o is reached such that $f(x_o) = x_o$. The value of input energy parameter k is taken equal to 4/3 following the argument given by equation (18). The results of integrations for the values of f_o, g_o, h_o and Q_o for $j = 2, k = 4/3$ and $\gamma = 7/5$ are given in Tables 1, 2, and 3 for $N = 10, 100, 1000$, respectively. The values of J_o and ξ_o come out to be 0.892782 and 0.773891, respectively.

4.2. Second approximation solution

As such the system of equations (21) cannot be integrated numerically because they contain an unknown ξ_1. Therefore, we write

$$f_1(x) = f_{11}(x) + \xi_1 f_{12}(x),$$

$$g_1(x) = g_{11}(x) + \xi_1 g_{12}(x),$$

$$h_1(x) = h_{11}(x) + \xi_1 h_{12}(x), \qquad (25)$$

$$Q_1(x) = Q_{11}(x) + \xi_1 Q_{12}(x).$$

$$\sigma_1 = \sigma_{11} + \xi_1 \sigma_{12}.$$

On substituting the equation (25) into equations (21) and (22) and then collecting the terms free from ξ_1, we get

$$0.5 f_{11} h_o - 0.5 f_o h_{11} + f_{11} h_o f_o^{'} - x\, h_{11} f_o^{'} + f_o h_{11} f_o^{'} - x\, h_o f_{11}^{'} + f_o h_o f_{11}' + g_{11}^{'}/\gamma = 0$$

$$2 f_{11} h_o / x + h_{11} + 2 f_o h_{11} / x + h_{11} f_o^{'} + h_o f_{11}^{'} + f_{11} h_o^{'} - x\, h_{11}^{'} + f_o h_{11}^{'} = 0 \qquad (26)$$

$$2\gamma\, f_{11} g_o / x + 2\gamma\, f_o g_{11} / x - 2\, Q_{11} / x + 2\gamma\, Q_{11} / x + \gamma\, g_{11} f_o^{'} + \gamma\, g_o f_{11}^{'} +$$
$$f_{11} g_o^{'} - x\, g_{11}^{'} + f_o g_{11}^{'} - Q_{11}^{'} + \gamma\, Q_{11}^{'} = 0$$

$$Q_{11}^{'} = 0$$

$$f_{11}(1) = -1/\gamma,\ g_{11}(1) = 0,\ h_{11}(1) = 0,\ Q_{11}(1) = 0 \qquad (27)$$

Equating the coefficients of ξ_1 on both sides of equations (21) and (22), we get

$$0.5 f_o h_o + 0.5 f_{12} h_o - 0.5 f_o h_{12} + f_{12} h_o f_o^{'} - x\, h_{12} f_o^{'} +$$
$$f_o h_{12} f_o^{'} - x\, h_o f_{12}^{'} + f_o h_o f_{12}^{'} + g_{12}^{'}/\gamma = 0$$

$$2 f_{12}h_o / x + h_{12} + 2 f_o h_{12} / x + h_{12} f_o' + h_o f_{12}' + f_{12}h_o' - x\, h_{12}' + f_o h_{12}' = 0$$

$$\begin{aligned} & g_o + 2\gamma\, f_{12}g_o / x + 2\gamma\, f_o g_{12} / x - 2\, Q_{12} / x + 2\gamma\, Q_{12} / x + \gamma\, g_{12} f_o' + \\ & \gamma\, g_o f_{12}' + f_{12}g_o' - x\, g_{12}' + f_o g_{12}' - Q_{12}' + \gamma\, Q_{12}' = 0 \end{aligned} \tag{28}$$

$$Q_{12}' = 0$$

$$f_{12}(1) = 0,\ g_{12}(1) = 0,\ h_{12}(1) = 0,\ Q_{12}(1) = 0 \tag{29}$$

The functions $f_{11}, g_{11}, h_{11}, Q_{11}, f_{12}, g_{12}, h_{12}$ and Q_{12} are obtained by numerical integration of equations (26) and (28) with the respective boundary conditions given by equations (27) and (29). If we know the values of these function and $f_o, g_o, h_o,$ and Q_o given in the tables 1, 2 and 3, the value of ξ_1 is obtained from the relation

$$\xi_1 = \frac{J_o\sigma_{11} - \int_{x_p}^{1}\left\{x^2(g_{11}/(\gamma-1) + f_o f_{11}h_o + 0.5\,(f_o)^2 h_{11})\right\}dx}{\int_{x_p}^{1}\left\{x^2(g_{12}/(\gamma-1) + f_o f_{12}h_o + 0.5\,(f_o)^2 h_{12})\right\}dx - J_o\sigma_{12}}, \tag{30}$$

where $\sigma_{11} = 0.933412$ and $\sigma_{12} = 1.400000$. The value of ξ_1 comes out to be -10135.1328616708. Now the functions f_1, g_1, h_1 and Q_1 calculated from equation (25) are given in Tables 4, 5, 6 for $j = 2, k = 4/3$, $\gamma = 7/5$ and different values of $N = 10, 100, 1000$, respectively.

4.3. Third approximation solution

The system of equations (23) cannot be integrated numerically because they involve an unknown ξ_2. Therefore, splitting the functions f_2, g_2, h_2 and Q_2 as:

$$f_2(x) = f_{21}(x) + \xi_2 f_{22}(x),$$

$$g_2(x) = g_{21}(x) + \xi_2 g_{22}(x),$$

$$h_2(x) = h_{21}(x) + \xi_2 h_{22}(x), \tag{31}$$

$$Q_2(x) = Q_{21}(x) + \xi_2 Q_{22}(x).$$

$$\sigma_2 = \sigma_{21} + \xi_2\sigma_{22}.$$

Substitution of the equation (31) into equations (23) and (24) gives the term free from ξ_2:

$$\begin{aligned} & \xi_1^2 f_o h_o - 0.5\xi_1 f_{11}h_o - 0.5\xi_1^2 f_{12}h_o + (3/2) f_{21}h_o + 0.5\xi_1 f_o h_{11} + 0.5 f_{11}h_{11} + 0.5\xi_1 f_{12}h_{11} + 0.5\xi_1^2 f_o h_{12} \\ & + 0.5\xi_1 f_{11}h_{12} + 0.5\xi_1^2 f_{12}h_{12} - 0.5 f_o h_{21} + f_{21}h_o f_o' + f_{11}h_{11} f_o' + \xi_1 f_{12}h_{11} f_o' + \xi_1 f_{11}h_{12} f_o' + \xi_1^2 f_{12}h_{12} f_o' \\ & - x\, h_{21} f_o' + f_o h_{21} f_o' + f_{11}h_o f_{11}' + \xi_1 f_{12}h_o f_{11}' - x\, h_{11} f_{11}' + f_o h_{11} f_{11}' - x\, \xi_1 h_{12} f_{11}' + \xi_1 f_o h_{12} f_{11}' + \xi_1 f_{11}h_o f_{12}' \\ & + \xi_1^2 f_{12}h_o f_{12}' - x\, \xi_1 h_{11} f_{12}' + \xi_1 f_o h_{11} f_{12}' - x\, \xi_1^2 h_{12} f_{12}' + \xi_1^2 f_o h_{12} f_{12}' - x\, h_o f_{21}' + f_o h_o f_{21}' + g_{21}'/\gamma = 0 \end{aligned}$$

$$2\, f_{21}h_o/x-\xi_1 h_{11}+2\, f_{11}h_{11}/x+2\,\xi_1 f_{12}h_{11}/x-\xi_1^2 h_{12}+2\,\xi_1 f_{11}h_{12}/x+2\,\xi_1^2 f_{12}h_{12}/x+$$
$$2\,h_{21}+2\, f_o h_{21}/x+h_{21}f_o^{'}+h_{11}f_{11}^{'}+\xi_1 h_{12}f_{11}^{'}+\xi_1 h_{11}f_{12}^{'}+\xi_1^2 h_{12}f_{12}^{'}+h_o f_{21}^{'}+f_{21}h_o^{'}+ \quad (32)$$
$$f_{11}h_{11}^{'}+\xi_1 f_{12}h_{11}^{'}+\xi_1 f_{11}h_{12}^{'}+\xi_1^2 f_{12}h_{12}^{'}-x\,h_{21}^{'}+f_o h_{21}^{'}=0$$

$$-2\,\xi_1^2 g_o+2\,\gamma\, f_{21}g_o/x+2\,\gamma\, f_{11}g_{11}/x+2\,\gamma\,\xi_1 f_{12}g_{11}/x+2\,\gamma\,\xi_1 f_{11}g_{12}/x+2\,\gamma\,\xi_1^2 f_{12}g_{12}/x$$
$$+g_{21}+2\,\gamma\, f_o g_{21}/x-2\,Q_{21}/x+2\,\gamma\,Q_{21}/x+\gamma\, g_{21}f_o^{'}+\gamma\, g_{11}f_{11}^{'}+\gamma\,\xi_1 g_{12}f_{11}^{'}+\gamma\,\xi_1 g_{11}f_{12}^{'}$$
$$+\gamma\,\xi_1^2 g_{12}f_{12}^{'}+\gamma\, g_o f_{21}^{'}+f_{21}g_o^{'}+f_{11}g_{11}^{'}+\xi_1 f_{12}g_{11}^{'}+\xi_1 f_{11}g_{12}^{'}+\xi_1^2 f_{12}g_{12}^{'}-x\,g_{21}^{'}+f_o g_{21}^{'}$$
$$-Q_{21}^{'}+\gamma\,Q_{21}^{'}=0$$

$$Q_{21}^{'}=0$$

$$f_{21}(1)=0,\ g_{21}(1)=0,\ h_{21}(1)=0,\ Q_{21}(1)=0.5\gamma^2 \quad (33)$$

From the coefficients of ξ_2

$$f_o h_o+1.5 f_{22}h_o-0.5 f_o h_{22}+f_{22}h_o f_o^{'}-x\,h_{22}f_o^{'}+f_o h_{22}f_o^{'}-x\,h_o f_{22}^{'}+g_{22}^{'}/\gamma=0$$

$$2\, f_{22}h_o/x+2\,h_{22}+2\, f_o h_{22}/x+h_{22}f_o^{'}+h_o f_{22}^{'}+f_{22}h_o^{'}-x\,h_{22}^{'}+f_o h_{22}^{'}=0 \quad (34)$$

$$2\,g_o+2\,\gamma\, f_{22}\,g_o/x+g_{22}+2\,\gamma\, f_o\,g_{22}/x-2\,Q_{22}/x+2\,\gamma\,Q_{22}/x+\gamma\, g_{22}f_o^{'}+\gamma\, g_o f_{22}^{'}+$$
$$f_{22}g_o^{'}-x\,g_{22}^{'}+f_o g_{22}^{'}-Q_{22}^{'}+\gamma\,Q_{22}^{'}=0$$

$$Q_{22}^{'}=0$$

$$f_{22}(1)=0,\ g_{22}(1)=0,\ h_{22}(1)=0,\ Q_{22}(1)=0 \quad (35)$$

Equations (32) and (34) are now integrated numerically with their respective boundary conditions given by equations (33) and (35). The value of ξ_2 is calculated from relation

$$\xi_2=\frac{J_o\sigma_{21}-\int_{x_p}^{1}\left\{\begin{array}{l}x^2(g_{21}/(\gamma-1)+0.5(f_{11})^2h_o+\xi_1 f_{11}f_{12}h_o+0.5\xi_1^2(f_{12})^2h_o+f_o f_{21}h_o\\+f_o f_{11}h_{11}+\xi_1 f_o f_{12}h_{11}+\xi_1 f_o f_{11}h_{12}+\xi_1^2 f_o f_{12}h_{12}+0.5(f_o)^2h_{21})\end{array}\right\}dx}{\int_{x_p}^{1}\left\{x^2(g_{22}/(\gamma-1)+f_o f_{22}h_o+0.5\,(f_o)^2h_{22})\right\}dx-J_o\sigma_{22}}, \quad (36)$$

where $\sigma_{21}=1.232651\times10^8$ and $\sigma_{22}=-1.285714$. The value of ξ_2 comes out to be 1.658964×10^{11}. The numerical values of the functions f_2, g_2, h_2 and Q_2 are given in Tables 7, 8 and 9 for $j=2, k=4/3$, $\gamma=7/5$ and different values of $N=10, 100, 1000$, respectively.

The non-dimensional expressions for the distribution of the pressure, the density, the particle velocity and the heat flux of radiation just behind the spherical shock wave in a radiating gas, correct up to third approximation are given by

$$\frac{p}{p_o} = \frac{1}{y}\left\{ g_o + g_1 y + g_2 y^2 \right\} \tag{37}$$

$$\frac{\rho}{\rho_o} = \left\{ h_o + h_1 y + h_2 y^2 \right\} \tag{38}$$

$$\frac{u}{a_o} = \frac{1}{\sqrt{y}}\left\{ f_o + f_1 y + f_2 y^2 \right\} \tag{39}$$

$$\frac{q}{p_o a_o} = \frac{1}{\sqrt[3]{y}}\left\{ Q_o + Q_1 y + Q_2 y^2 \right\} \tag{40}$$

Table 1 First approximate solution for $k = 4/3$, $\gamma = 7/5$ and $N = 10$

x	f_o	g_o	h_o	Q_o
0.9076	1.11047	0.99998	0.00042	-0.5
0.9153	1.09971	0.99998	0.00040	-0.5
0.9230	1.08926	0.99998	0.00038	-0.5
0.9307	1.07912	0.99998	0.00036	-0.5
0.9384	1.06928	0.99999	0.00034	-0.5
0.9461	1.05971	0.99999	0.00032	-0.5
0.9538	1.05042	0.99999	0.00030	-0.5
0.9615	1.0414	0.99999	0.00027	-0.5
0.9692	1.03264	0.99999	0.00025	-0.5
0.9769	1.02412	0.99999	0.00021	-0.5
0.9846	1.01585	0.99999	0.00017	-0.5
0.9923	1.00781	1	0.00012	-0.5
1	1	1	0	-0.5

Table 2 First approximate solution for $k = 4/3$, $\gamma = 7/5$ and $N = 100$

x	f_o	g_o	h_o	Q_o
0.9076	6.40023×10^{22}	-2.24066×10^{22}	3.30679×10^{27}	-0.5
0.9153	4.92981×10^{22}	-1.72588×10^{22}	2.54707×10^{27}	-0.5
0.9230	3.70384×10^{22}	-1.29668×10^{22}	1.91365×10^{27}	-0.5
0.9307	2.7001×10^{22}	-9.45277×10^{21}	1.39505×10^{27}	-0.5
0.9384	1.89636×10^{22}	-6.63898×10^{21}	9.79789×10^{26}	-0.5
0.9461	1.27042×10^{22}	-4.4476×10^{21}	6.56382×10^{26}	-0.5

0.9538	8.00029×10^{21}	-2.80082×10^{21}	4.13349×10^{26}	-0.5
0.9615	4.6298×10^{21}	-1.62084×10^{21}	2.39206×10^{26}	-0.5
0.9692	2.37046×10^{21}	-8.29872×10^{20}	1.22474×10^{26}	-0.5
0.9769	1.00004×10^{21}	-3.50102×10^{20}	5.16686×10^{25}	-0.5
0.9846	2.96307×10^{20}	-1.03734×10^{20}	1.53092×10^{25}	-0.5
0.9923	3.70384×10^{19}	-1.29668×10^{19}	1.91365×10^{24}	-0.5
1	1	1	0	-0.5

Table 3 First approximate solution for $k = 4/3,\ \gamma = 7/5$ and $N = 1000$

x	f_o	g_o	h_o	Q_o
0.9076	6.40023×10^{22}	-2.23842×10^{22}	3.32733×10^{27}	-0.5
0.9153	4.92981×10^{22}	-1.72415×10^{22}	2.56289×10^{27}	-0.5
0.9230	3.70384×10^{22}	-1.29538×10^{22}	1.92554×10^{27}	-0.5
0.9307	2.7001×10^{22}	-9.44334×10^{21}	1.40372×10^{27}	-0.5
0.9384	1.89636×10^{22}	-6.63236×10^{21}	9.85875×10^{26}	-0.5
0.9461	1.27042×10^{22}	-4.44316×10^{21}	6.60459×10^{26}	-0.5
0.9538	8.00029×10^{21}	-2.79803×10^{21}	4.15916×10^{26}	-0.5
0.9615	4.6298×10^{21}	-1.61923×10^{21}	2.40692×10^{26}	-0.5
0.9692	2.37046×10^{21}	-8.29045×10^{20}	1.23234×10^{26}	-0.5
0.9769	1.00004×10^{21}	-3.49753×10^{20}	5.19895×10^{25}	-0.5
0.9846	2.96307×10^{20}	-1.03631×10^{20}	1.54043×10^{25}	-0.5
0.9923	3.70384×10^{19}	-1.29538×10^{19}	1.92554×10^{24}	-0.5
1	1	1	0	-0.5

Table 4 Second approximate solution for $k = 4/3, \gamma = 7/5$ and $N = 10$

x	f_1	g_1	h_1	Q_1
0.9076	-596.856	-1989.44	42504.8	0.00416
0.9153	-567.197	-1626.75	39209.1	0.00399
0.9230	-530.540	-1308.88	35869.3	0.00381
0.9307	-488.216	-1032.66	32485.0	0.00363
0.9384	-441.383	-795.109	29056.3	0.00343
0.9461	-391.050	-593.506	25582.7	0.00322
0.9538	-338.090	-425.327	22064.0	0.00298

0.9615	-283.254	-288.247	18500.3	0.00273
0.9692	-227.195	-180.121	14891.4	0.00245
0.9769	-170.468	-98.9743	11237.0	0.00212
0.9846	-113.551	-42.9931	7536.91	0.00174
0.9923	-56.8516	-10.5108	3791.19	0.00123
1	-0.71429	0	0	0

Table 5 Second approximate solution for $k = 4/3$, $\gamma = 7/5$ and $N = 100$

x	f_1	g_1	h_1	Q_1
0.9076	-2.40350×10^{31}	-2.54629×10^{25}	2.38602×10^{33}	3.30678×10^{29}
0.9153	-1.85131×10^{31}	-1.96130×10^{25}	1.83784×10^{33}	2.54706×10^{29}
0.9230	-1.39092×10^{31}	-1.47355×10^{25}	1.38079×10^{33}	1.91364×10^{29}
0.9307	-1.01398×10^{31}	-1.07422×10^{25}	1.00660×10^{33}	1.39505×10^{29}
0.9384	-7.12149×10^{30}	-7.54458×10^{24}	7.06968×10^{32}	9.79785×10^{28}
0.9461	-4.77085×10^{30}	-5.05428×10^{24}	4.73613×10^{32}	6.5638×10^{28}
0.9538	-3.00438×10^{30}	-3.18287×10^{24}	2.98252×10^{32}	4.13347×10^{28}
0.9615	-1.73864×10^{30}	-1.84194×10^{24}	1.72600×10^{32}	2.39205×10^{28}
0.9692	-8.90185×10^{29}	-9.43073×10^{23}	8.83709×10^{31}	1.22473×10^{28}
0.9769	-3.75547×10^{29}	-3.97858×10^{23}	3.72815×10^{31}	5.16684×10^{27}
0.9846	-1.11273×10^{29}	-1.17884×10^{23}	1.10463×10^{31}	1.53091×10^{27}
0.9923	-1.39092×10^{28}	-1.47355×10^{22}	1.38079×10^{30}	1.91364×10^{26}
1	-0.71429	0	0	0

Table 6 Second approximate solution for $k = 4/3$, $\gamma = 7/5$ and $N = 1000$

x	f_1	g_1	h_1	Q_1
0.9076	-2.50363×10^{31}	-9.58934×10^{24}	2.40169×10^{33}	3.32731×10^{30}
0.9153	-1.92843×10^{31}	-7.38623×10^{24}	1.84991×10^{33}	2.56288×10^{30}
0.9230	-1.44886×10^{31}	-5.54940×10^{24}	1.38987×10^{33}	1.92553×10^{30}
0.9307	-1.05622×10^{31}	-4.04551×10^{24}	1.01321×10^{33}	1.40371×10^{30}
0.9384	-7.41816×10^{30}	-2.84129×10^{24}	7.11612×10^{32}	9.85871×10^{29}

0.9461	-4.96959×10^{30}	-1.90343×10^{24}	4.76724×10^{32}	6.60456×10^{29}
0.9538	-3.12954×10^{30}	-1.19867×10^{24}	3.00211×10^{32}	4.15914×10^{29}
0.9615	-1.81107×10^{30}	-6.93678×10^{23}	1.73733×10^{32}	2.40691×10^{29}
0.9692	-9.27270×10^{29}	-3.55162×10^{23}	8.89515×10^{31}	1.23234×10^{29}
0.9769	-3.91192×10^{29}	-1.49834×10^{23}	3.75265×10^{31}	5.19893×10^{28}
0.9846	-1.15909×10^{29}	-4.43956×10^{22}	1.11189×10^{31}	1.54042×10^{28}
0.9923	-1.44886×10^{28}	-5.54940×10^{21}	1.38987×10^{30}	1.92553×10^{27}
1	-0.71429	0	0	0

Table 7 Third approximate solution for $k=4/3$, $\gamma=7/5$ and $N=10$

x	f_2	g_2	h_2	Q_2
0.9076	24298278178.49	-1729674816	44707995800	425057
0.9153	22051787217.76	-1354181988	39608761680	392099
0.9230	19853515084.48	-1038825028	34642040360	358699
0.9307	17700622913.28	-777654012	29847935800	324855
0.9384	15590313663.96	-563830896.80	25232966360	290566
0.9461	13520206396.52	-393851511.20	20823706240	255828
0.9538	11488158023.56	-261033443.60	16674992680	220642
0.9615	9492249401.400	-161090064.80	12778364240	185005
0.9692	7530756349.560	-89802240.000	9204833760	148914
0.9769	5602100495.000	-42459586.360	6007439864	112370
0.9846	3704912141.120	-14911697.880	3281055148	75369.5
0.9923	1837918388.360	-2502641.1440	1154742964	37912.1
1	0	0	0	0.25510

Table 8 Third approximate solution for $k=4/3$, $\gamma=7/5$ and $N=100$

x	f_2	g_2	h_2	Q_2
0.9076	7.83135×10^{38}	7.67538×10^{32}	9.21162×10^{38}	2.38602×10^{35}

0.9153	6.03214×10^{38}	5.91200×10^{32}	7.09529×10^{38}	1.83784×10^{35}
0.9230	4.53204×10^{38}	4.44177×10^{32}	5.33079×10^{38}	1.3808×10^{35}
0.9307	3.30385×10^{38}	3.23804×10^{32}	3.88616×10^{38}	1.0066×10^{35}
0.9384	2.32040×10^{38}	2.27419×10^{32}	2.72937×10^{38}	7.06968×10^{34}
0.9461	1.55448×10^{38}	1.52353×10^{32}	1.82846×10^{38}	4.73613×10^{34}
0.9538	9.78920×10^{37}	9.59423×10^{31}	1.15144×10^{38}	2.98252×10^{34}
0.9615	5.66504×10^{37}	5.55221×10^{31}	6.66345×10^{37}	1.726×10^{34}
0.9692	2.90051×10^{37}	2.84273×10^{31}	3.41170×10^{37}	8.8371×10^{33}
0.9769	1.22365×10^{37}	1.19928×10^{31}	1.43931×10^{37}	3.72815×10^{33}
0.9846	3.62562×10^{36}	3.55342×10^{30}	4.26464×10^{36}	1.10464×10^{33}
0.9923	4.53204×10^{35}	4.44177×10^{29}	5.33078×10^{35}	1.3808×10^{32}
1	0	0	0	0.255102

Table 9 Third approximate solution for $k=4/3$, $\gamma=7/5$ and $N=1000$

x	f_2	g_2	h_2	Q_2
0.9076	7.87383×10^{38}	7.72307×10^{32}	9.28112×10^{38}	2.40169×10^{36}
0.9153	6.06485×10^{38}	5.94873×10^{32}	7.14880×10^{38}	1.84991×10^{36}
0.9230	4.55662×10^{38}	4.46937×10^{32}	5.37101×10^{38}	1.38987×10^{36}
0.9307	3.32176×10^{38}	3.25816×10^{32}	3.91547×10^{38}	1.01321×10^{36}
0.9384	2.33299×10^{38}	2.28832×10^{32}	2.74995×10^{38}	7.11612×10^{35}
0.9461	1.56292×10^{38}	1.53299×10^{32}	1.84226×10^{38}	4.76725×10^{35}
0.9538	9.84227×10^{37}	9.65383×10^{31}	1.16015×10^{38}	3.00211×10^{35}
0.9615	5.69575×10^{37}	5.58670×10^{31}	6.71375×10^{37}	1.73733×10^{35}
0.9692	2.91622×10^{37}	2.86039×10^{31}	3.43746×10^{37}	8.89515×10^{34}
0.9769	1.23028×10^{37}	1.20672×10^{31}	1.45017×10^{37}	3.75264×10^{34}
0.9846	3.64528×10^{36}	3.57549×10^{30}	4.29682×10^{36}	1.11189×10^{34}
0.9923	4.55662×10^{35}	4.46937×10^{29}	5.37101×10^{35}	1.38987×10^{33}
1	0	0	0	0.255102

5. Results and Discussion

In the present paper the power series similarity solutions for spherical shock waves of variable energy in a radiating atmosphere are presented. The goal of the present investigation was to examine the effect due to the radiation parameter on the flow variables in the region just behind the spherical shock front. The non-dimensional forms of the expressions for the distribution of the pressure p/p_o, the density ρ/ρ_o, the particle velocity u/a_o and the heat flux of radiation $q/p_o a_o$ just behind the spherical shock front in a radiating gas are given by equations (37) – (40), respectively. These non-dimensional expressions for the flow quantities are the functions of the propagation distance *x* from the origin O, the adiabatic index γ, the energy-input parameter *k*, the inverse of the square of Mach number *y* and the radiation-parameter *N* of the medium. For the purpose of numerical computation the values of parameters are taken to be $\gamma = 7/5$, $k = 4/3$, $y = 0.1, 0.15, 0.20, 0.25$ and $N = 10,100,1000$. It is very useful to mention that the present analysis serves a description for the propagation of strong exploding spherical shock waves through an in-viscid, non-heat conducting and electrically infinitely conducting radiating fluids. The variations of the pressure, the density, the particle velocity and the heat flux of radiation with the distance *x* for $k = 4/3$, $N = 10$, $\gamma = 7/5$ and different values of *y* are shown in figure 1. It is remarkable that just behind the shock the pressure decreases with increase in the distance *x* from the shock front and it also decreases with increase in the value of *y*. The density, the particle velocity and the heat flux of radiation just behind the shock front increase with increase in the distance *x* from the shock front and also with increase in the value of *y*. Figure 2 shows the variations of the pressure, the density, the particle velocity and the heat flux of radiation with distance *x* for $\beta = 4/3$, $y = 0.25$, $\gamma = 7/5$ and different values of N. It is noteworthy that just behind the shock front the heat flux of radiation increases with increase in the distance *x* from the shock front rapidly for $N = 1000$ and slowly for $N = 100$ while remains unchanged for $N = 10$. The pressure, the density and the particle velocity just behind the shock front increase with the distance *x* from the shock front for $N \geq 100$ while remain almost unchanged for $N = 10$. It is important to note that the pressure, the density, the particle velocity and the heat flux of radiation increase with increase in the value of radiation parameter *N*. Thus, the radiation parameter *N* affects the variations of the pressure, the density, the particle velocity and the heat flux of radiation as its value increases.

6. Conclusions

In this paper the power series similarity solutions for spherical shock waves are extended by accounting for radiation. The investigations made in the paper are intended to contribute to the understanding of the strong exploding shock waves in radiating astrophysical fluids by giving, for the first time, the power series similarity solutions for the flow field behind the exploding spherical shock front. The effects due to the radiation parameter on the flow-field behind the strong exploding spherical shock wave were studied in view of the Rosseland's radiative diffusion model [20].

The following conclusions may be drawn from the findings of the current analysis:

1. The pressure decreases with increase in the value of *y* while the density, the particle velocity and the heat flux of radiation increase just behind the spherical shock front.

2. The pressure, the density, the particle velocity and the heat flux of radiation just behind the spherical shock front increase with increase in the value of radiation parameter.

Such problem is of great interest in astrophysics and space science as it is highly relevant in order to understand the processes which take place in the stellar media and to explain the observed luminosity of stars. To a large extent, this theory can also be applied to other high temperature systems considered in modern physics and engineering where the heat flux of radiation plays an important role. The present findings can be applied to normal stars, to exploding stars or stars with violent winds, to active galaxies, and on Earth wherever matter is very hot.

References

1. Shull J M and McKee C F 1979 Theoretical Models of Interstellar Shocks. I. Radiative Transfer and Ultraviolet Precursors J. Astrophys. 227 131-49

2. Blondin J M, Wright E B, Borkowski K J and Reynolds S P 1998 Transition to the radiative phase in supernova remnants J. Astrophys. 500 342-54

3. Stokes G 1851 An examination of the possible effect of the radiation of heat on the propagation of sound Phil. Mag. 1, 305-17

4. Sachs R G 1946 Some properties of very intense shock waves Phys. Rev. 69 514 - 22

5. Guess A W and Sen H K 1958 Radiation effects on Rankine Hugoniot Shock conditions, Conference on Extremely high temperatures (New York: John Wiley)

6. Sen H K and Guess A W 1957 Radiation effects in shock-wave structure Phys. Rev. 108 (3) 560 - 4

7. Zeldovich Ya B and Raizer Yu P 2002 Physics of Shock Waves and High Temperature Hydrodynamics Phenomena (New York: Dover)

8. Mihalas D and Mihalas B W 1999 Foundations of Radiation Hydrodynamics (New York: Dover)

9. Marshak R E 1958 Effect of radiation on shock wave behaviour Phys. Fluids 1(1) 24–9

10. Elliott L A 1960 Similarity methods in radiation hydrodynamics Proc. R. Soc. Lond. A 258(3) 287–301

11. Wang K C 1964 The piston problem with thermal radiation Fluid Mech. 20(3) 447–55

12. Helliwell J B 1969 Self-similar piston problem with radiative heat transfer Fluid Mech. 37(3) 497–512

13. Laumbach D and Probstein R F 1970 A point explosion in a cold exponential atmosphere- Part 2, Radiating flow Fluid Mech. 40(4) 833–58

14. Laumbach D and Probstein R F 1970 Self-similar strong shocks with radiation in a decreasing exponential atmosphere Phys. Fluids 13 1178-83

15. Bhowmick J B 1981 An exact analytical solution in radiation gas dynamics Astrophys. Space Sci. 74 (2) 481-5

16. Singh J B and Srivastava S K 1982 Propagation of spherical shock waves in an exponential medium with radiation heat flux Astrophys. Space Sci, 88 (2) 277-82

17. Ghoniem A F, Kamel M M, Berger S A and Oppenheim A K 1982 Effects of internal heat transfer on the structure of self-similar blast waves Fluid Mech. 117 473–91

18. Gretler W and Wehle P 1993 Propagation of blast waves with exponential heat release and internal heat conduction and thermal radiation Shock Waves 3(2) 95–104

19. Anand R K 2018 On the strong spherical shock waves in a two-phase gas-particle medium Int. J. Appl. Comput. Math. 4 (1) 49 14pp

20. Pomraning G C 1973 The Equations of Radiation Hydrodynamics, Int. Ser. Monographs in natural philosophy 54 (New York: Pergamon)

21. Freeman R A 1968 Variable energy blast wave J. Phys. D: Appl. Phys. 1 1697-1710

22. Wang K C 1966 Approximate solution of a plane radiating piston problem Phys. Fluids 9 (10) 1922-8

23. Sakurai A 1953 On the Propagation and Structure of the Blast Wave I J. Phys. Soc. Japan 8 (5) 662-9

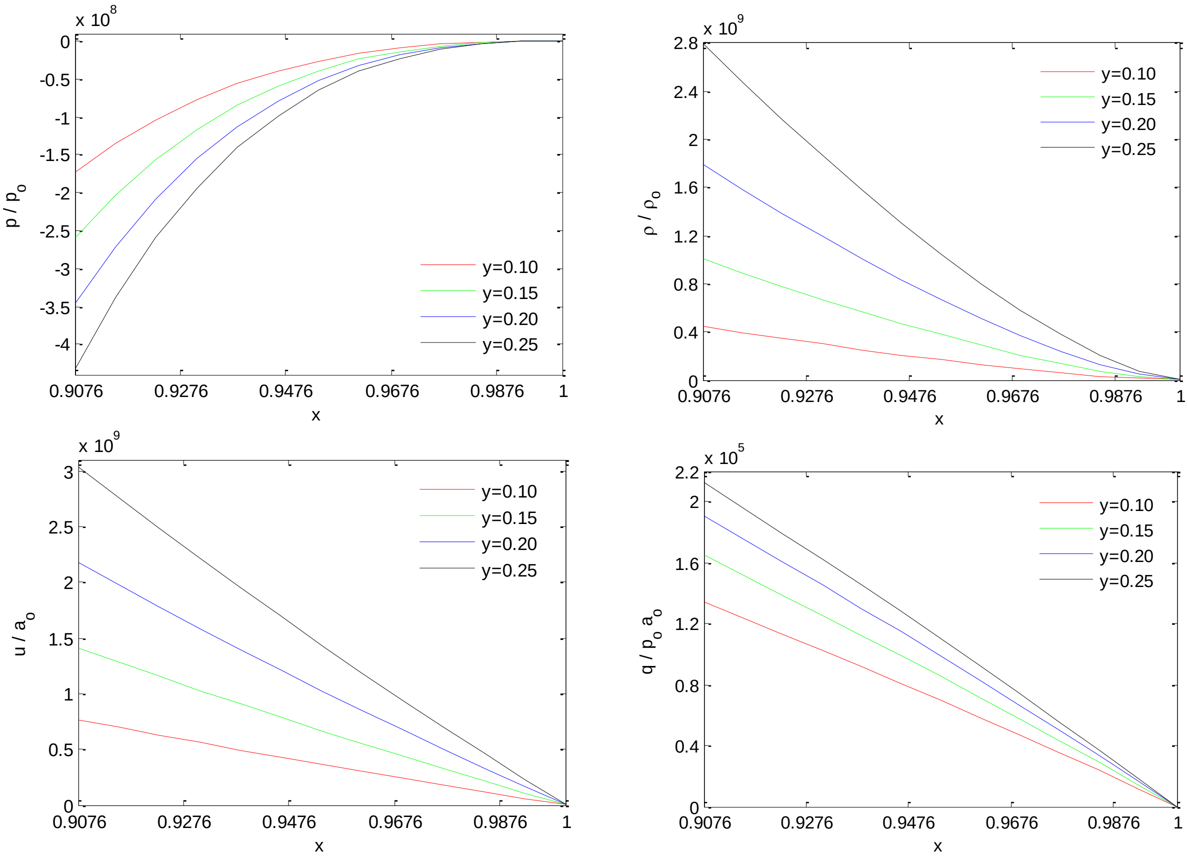

Figure 1. Non-dimensional pressure, density, particle velocity and heat flux radiation distribution behind spherical shock wave with propagation distance for $k = 4/3$, $N = 10$, $\gamma = 7/5$ and different values of y .

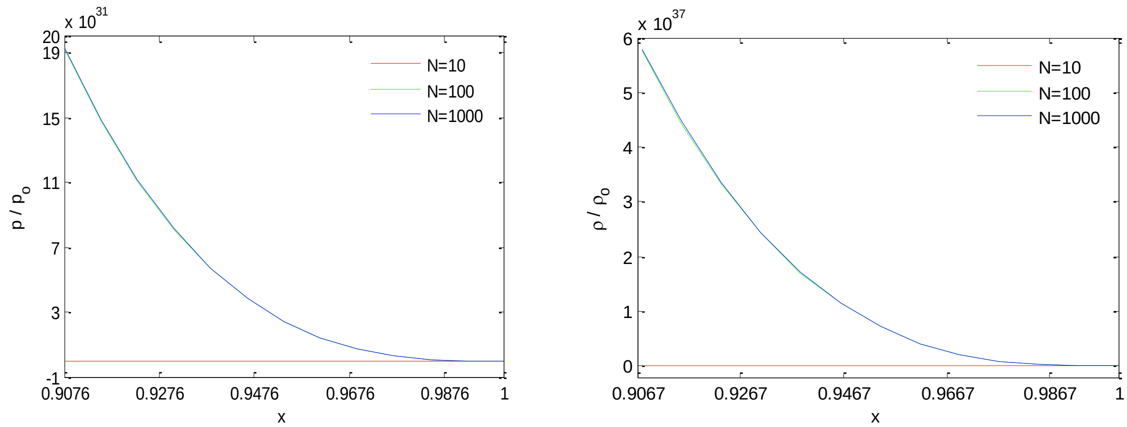

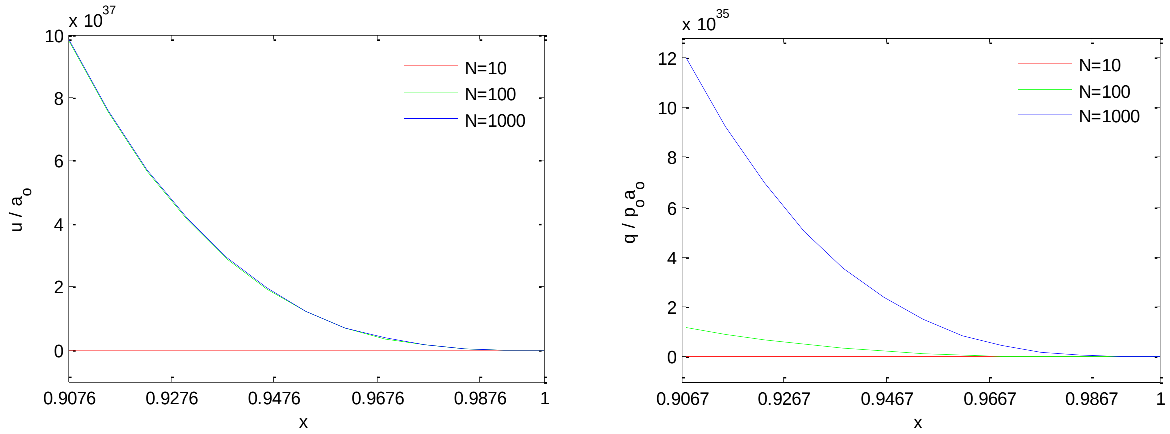

Figure 2. Non-dimensional pressure, density, particle velocity and heat flux radiation distribution behind spherical shock wave with propagation distance for $k = 4/3$, $y = 0.25$, $\gamma = 7/5$ and different values of radiation parameter.